EARTHQUAKE RESPONSE ANALYSIS FOR JAPANESE TRADITIONAL WOODEN BUILDINGS WITH MUD WALLS USING SEMI-RIGID FRAME MODEL

S. Matsumoto [1] and Y. Suzuki[2]

[1] *Assistant Professor, Dept. of Social and Environmental Engineering, Hiroshima University, Japan*
Email: mshin@hiroshima-u.ac.jp
[2] *Professor, Disaster Prevention Research Institute, Kyoto University, Japan*
Email: suzuki@zeisei.dpri.kyoto-u.ac.jp

ABSTRACT :

It is carried out the vibration test for full scale building by large three-dimensional shaking table in recent years. In this paper, we compare the present earthquake response analysis with full-scale vibration test for Japanese traditional wooden building on Hyogo Earthquake Engineering Research Center 'E-defense' in 2006. Those traditional wooden buildings have mud walls for earthquake resisting element. Then, we illustrate the modeling for mud walls and the beam-column joints using on the semi-rigid frame analysis. And, we investigate the validity of this modeling and characteristics of the solution on earthquake response for Japanese traditional wooden buildings.

KEYWORDS: Japanese traditional wooden buildings, semi-rigid frame, mud walls, earthquake response analysis, frame analysis

1. INTRODUCTION

It has not been clarified that the structure-mechanical characteristics for the traditional wooden buildings because of the horizontal plane of structure such as roof or floor construction, the foundation stone of column base which does not hold the waist tie beam, Orthogonal vertical plane of structure, and complicated joints such as the connected beam to column and so on. The vibration test was carried out at the E-defense (Hyogo Earthquake Engineering Research Center) to clear the effect of seismic response characteristic and earthquake resisting performance for traditional wooden buildings. In this study, we remarked the particularity for tradition construction method on the column base and floor plane of structure.

In this paper, we illustrate the modeling for mud walls and the beam-column joints using on the semi-rigid frame analysis. The mud wall element is formulated by the composite elements consist of one horizontal nonlinear spring element and three rigid beams pined other elements. The nonlinear characteristics of walls and beam-column joints are evaluated by slip-bilinear relationship model obtained from previous experimental studies, respectively. In addition, we formulated the slip phenomenon for the column base on foundation stone observed in Japanese wooden buildings by shearing spring element. The nonlinear characteristic of the shearing spring element is assumed by Coulomb friction model. And we discuss the relationship between coefficient of friction in numerical analysis and the physical phenomenon in full-scale vibration test. We investigate the validity of this modeling and characteristics of the solution on earthquake response for Japanese traditional wooden buildings.

2. THE OUTLINE OF NUMERICAL METHOD

In this paper, the nonlinear characteristic of connection in the traditional wooden buildings is modeling by the semi-rigid beam element shown in Figure 1. The relationship (M-θ relation) between

bending moment and relative rotation angle of the column-beam joint is evaluated by slip bilinear restoring force characteristics based on previous experimental tests.

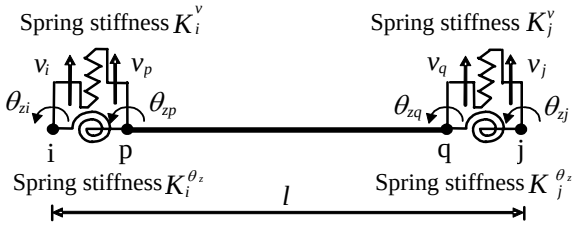

Figure 1 The coordinate system of semi-rigid beam element

An equation of motion of the element with length zero spring elements are given as follows.

$$[m_v]\{\ddot{v}\}+[c_v]\{\dot{v}\}+[k_v]\{v\}=\{f_y\} \tag{2.1}$$

Where

$$[m_v]=\rho Al\begin{bmatrix}0 & & & & & & & \text{Sym.}\\ 0 & 0 & & & & & & \\ 0 & 0 & \frac{13}{35} & & & & & \\ 0 & 0 & \frac{11l}{210} & \frac{l^2}{105} & & & & \\ 0 & 0 & \frac{9}{70} & \frac{13l}{420} & \frac{13}{35} & & & \\ 0 & 0 & \frac{-13l}{420} & \frac{-l^2}{140} & \frac{-11l}{210} & \frac{l^2}{105} & & \\ 0 & 0 & 0 & 0 & 0 & 0 & 0 & \\ 0 & 0 & 0 & 0 & 0 & 0 & 0 & 0\end{bmatrix},\quad [k_v]=\begin{bmatrix}K_i^v & & & & & & & \text{Sym.}\\ 0 & K_i^{\theta_z} & & & & & & \\ -K_i^v & 0 & \frac{12EI_z}{l^3}+K_i^v & & & & & \\ 0 & -K_i^{\theta_z} & \frac{6EI_z}{l^2} & \frac{4EI_z}{l}+K_i^{\theta_z} & & & & \\ 0 & 0 & -\frac{12EI_z}{l^3} & -\frac{6EI_z}{l^2} & \frac{12EI_z}{l^3}+K_j^v & & & \\ 0 & 0 & \frac{6EI_z}{l^2} & \frac{2EI_z}{l} & -\frac{6EI_z}{l^2} & \frac{4EI_z}{l}+K_j^{\theta_z} & & \\ 0 & 0 & 0 & 0 & -K_j^v & 0 & K_j^v & \\ 0 & 0 & 0 & 0 & 0 & -K_j^{\theta_z} & 0 & K_j^{\theta_z}\end{bmatrix}$$

$$\{v\}^T=\begin{bmatrix}v_i & \theta_{zi} & v_p & \theta_{zp} & v_q & \theta_{zq} & v_j & \theta_{zj}\end{bmatrix},\quad \{f_y\}^T=\begin{bmatrix}f_{yi} & m_{zi} & 0 & 0 & 0 & 0 & f_{yj} & m_{zj}\end{bmatrix}$$

Then, $(\dot{})$ shows the time derivative. ρ is the unit volume mass of the element, and A is the cross section of the member. And the damping is assumed in proportional to the initial stiffness as $[C_v]=2h_1/\omega_1[k_v]$. ω_1 is the first natural circular frequency. h_1 is a damping factor of the first mode. v_i is the deflection and θ_{zi} is the rotational angle around *z*-axis at the mode *i*. f_{yi} is the nodal shearing force and m_{zi} is the nodal bending moment at the node *i*.

Next, we transform the Eqn. 2.1 by applying static condensation technique as the following procedure. In the first place, by taking out from 3 lines to 6 lines in the equation Eqn. 2.1, The following equation is derived.

$$\left[m_v^{pq}\right]\left\{\ddot{v}^{pq}\right\}+\frac{2h_1}{\omega_1}\left(\left[\bar{k}_v^{pq}\right]\left\{\dot{v}^{pq}\right\}-\left[s_v\right]\left\{\dot{v}^{ij}\right\}\right)+\left[\bar{k}_v^{pq}\right]\left\{v^{pq}\right\}-\left[s_v\right]\left\{v^{ij}\right\}=\{0\} \tag{2.2}$$

Where

$$[s_v]=\begin{bmatrix}K_i^v & & & \text{Sym.}\\ 0 & K_i^{\theta_z} & & \\ 0 & 0 & K_j^v & \\ 0 & 0 & 0 & K_j^{\theta_z}\end{bmatrix},\quad \left\{v^{pq}\right\}^T=\begin{bmatrix}v_p & \theta_{zp} & v_q & \theta_{zq}\end{bmatrix},\quad \left\{v^{ij}\right\}^T=\begin{bmatrix}v_i & \theta_{zi} & v_j & \theta_{zj}\end{bmatrix}$$

In the second place, Eqn. 2.2 is expressed as follows.

$$\left[m_v^{pq}\right]\left(\left\{\ddot{v}^{pq}\right\}-\left[\bar{k}_v^{pq}\right]^{-1}\left[s_v\right]\left\{\ddot{v}^{ij}\right\}\right)+\frac{2h_1}{\omega_1}\left[\bar{k}_v^{pq}\right]\left(\left\{\dot{v}^{pq}\right\}-\left[\bar{k}_v^{pq}\right]^{-1}\left[s_v\right]\left\{\dot{v}^{ij}\right\}\right)$$
$$+\left[\bar{k}_v^{pq}\right]\left(\left\{v^{pq}\right\}-\left[\bar{k}_v^{pq}\right]^{-1}\left[s_v\right]\left\{v^{ij}\right\}\right)=-\left[m_v^{pq}\right]\left[\bar{k}_v^{pq}\right]^{-1}\left[s_v\right]\left\{\ddot{v}^{ij}\right\} \tag{2.3}$$

Though the right-hand side of Eqn. 2.3 is not generally zero, if it is handled that the mass system assumed the lumped mass system, the right-hand side is equal to exactly zero. Then, we treat the right-hand side of Eqn 2.3 as zero. Therefore, application scope of this formulation is lumped mass system problem only. The following equation is derived from Eqn. 2.3.

$$\left\{\ddot{v}\right\}=\left[T_v\right]\left\{\ddot{v}^{ij}\right\},\ \left\{\dot{v}\right\}=\left[T_v\right]\left\{\dot{v}^{ij}\right\},\ \left\{v\right\}=\left[T_v\right]\left\{v^{ij}\right\} \tag{2.4}$$

Where

$$\underset{8\times 4}{\left[T_v\right]}=\begin{bmatrix}1&0&0&0\\0&1&0&0\\\left[\bar{k}_v^{pq}\right]^{-1}\left[s_v\right]\\0&0&1&0\\0&0&0&1\end{bmatrix}$$

By substituting Eqn. 2.1 for Eqn. 2.4 energetically, the contracted equation of motion is obtained as follows.

$$\left[T_v\right]^T\left[m_v\right]\left[T_v\right]\left\{\ddot{v}^{ij}\right\}+\frac{2h_1}{\omega_1}\left[T_v\right]^T\left[k_v\right]\left[T_v\right]\left\{\dot{v}^{ij}\right\}+\left[T_v\right]^T\left[k_v\right]\left[T_v\right]\left\{v^{ij}\right\}=\left[T_v\right]^T\left\{f_y\right\} \tag{2.5}$$

When the rigid connections are included, the following equation

$$\left[k_v\right]\left\{v^{pq}\right\}-\left[s_v\right]\left\{v^{ij}\right\}=\left\{0\right\} \tag{2.6}$$

is changed to satisfy the rigid conditions for $v_p = v_i \cdots$. etc.

In the same way, we can formulate the equations of motion for bending deformation around *x*-axis, axial deformation, and torsional deformation.

The wall element is formulated by one translation spring element for the story deformation angle shown in Figure 2. The nonlinear characteristics of mud wall are formulated by slip bilinear restoring force characteristics resulted from previous studies.

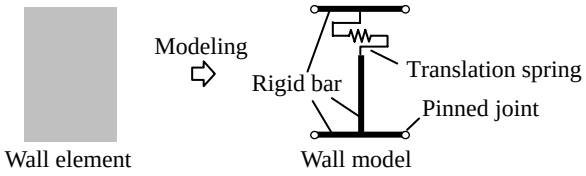

Figure 2 The wall model (rocking rigid body model)

The numerical integration of the equation of motion for earthquake response analysis is used Newmark's β method (β=1/4 in this numerical examples). The increment interval time Δt was Δt=0.001 sec., and damping characteristic of the structure was assumed the initial stiffness proportion damping (damping factor h=0.05 in this numerical examples).

3. NUMERICAL EXAMPLES

In this paper, the numerical examples were respectively calculated for 2 kinds of Model A "sill beam type" (See Figure 3) and Model B "waist tie beam type" (See Figure 4). The horizontal plane of structure at the roof floor is handled by the brace element as a rigid body to each frame unit.

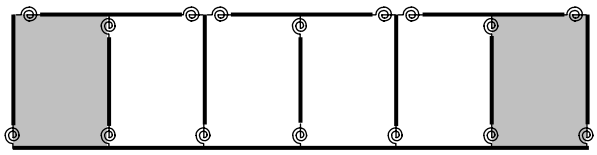

Figure 3 Model A (sill beam type)
(elevation plan for long edge direction)

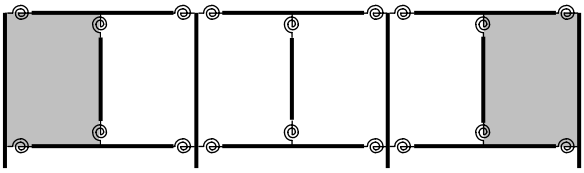

Figure 4 Model B (waist tie beam type)
(elevation plan for long edge direction)

The mud wall was in the each building corner along the long edge direction, as shown in Figure 5, and these models were eccentric wall layout for short edge direction (at X1 plane of structure). The wall element consist of 3 rigid bar elements and pinned connections and one shear spring element for horizontal direction, as shown in Figures 6.

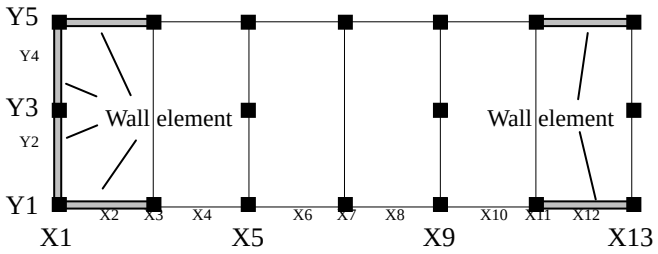

Figure 5 The wall layout (plan figure)

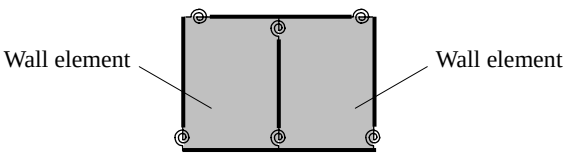

Elevation plan for short edge direction
（plane of structure X1）

Figure 6 Modeling of the wall

4. THE RESULT OF ANALYSIS

The figures of vibrational mode obtained from eigenvalue analysis are shown in Figures 7. Then, the first natural frequency for the Model A (sill beam type) was 0.65Hz, and Model B (waist tie beam type) was 0.74Hz.

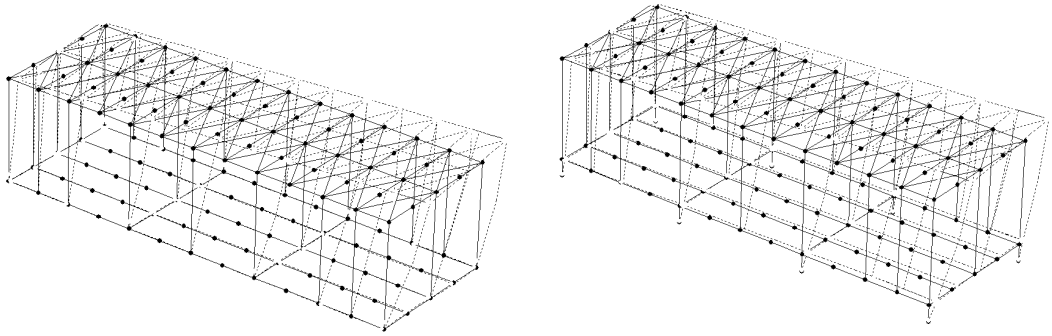

Model A (sill beam type) : 0.65Hz Model B (waist tie beam type) : 0.74Hz

Figure 7 Vibrational mode (1st mode)

In the case of inputting BCJ-L2 (The Building Center of Japan, Level 2) wave into the Model A (sill beam type) for the short edge direction, the largest deformation angle at main vertical plane of structure and the maximum acceleration at main vertical plane of structure top are shown in Figures 8 and Figures 9. In these figures, the continuous line shows analysis value, and the dotted line shows experimental value.

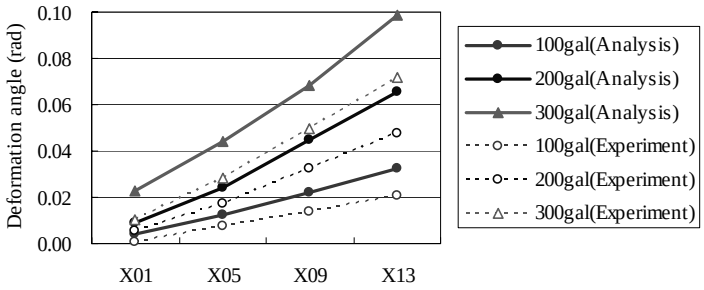

Figure 8 The largest deformation angle

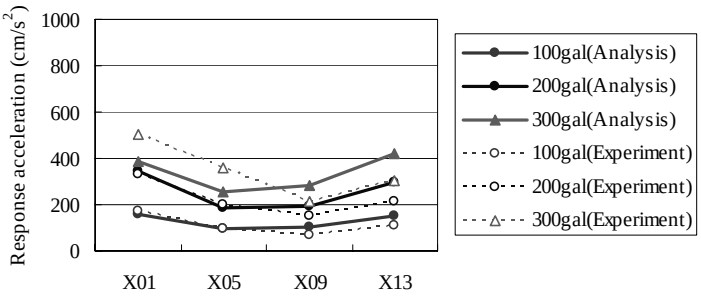

Figure 9 The largest response acceleration

The story deformation angle of X13 plane of structure inputted BCJ-L2 wave 300gal is shown in Figures 10. In this figure, the black line shows analysis value, and the gray line shows experimental value. This figure shows the good correspondence between experimental value and analysis value.

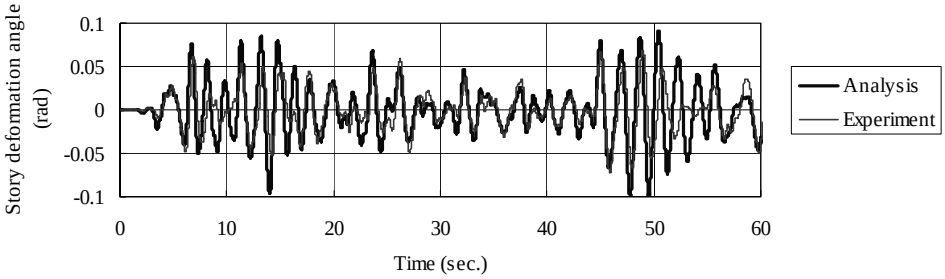

Figure 10 The story deformation angle of X13 plane of structure (BCJ-L2, 300gal)

On the other hand, for Model B (waist tie beam) type building, the slip phenomenon between column base and foundation stone was considered. These slip properties are expressed by shear spring at the column base, as shown in Figure 11. In this analysis, the friction coefficient μ was made to be μ =0.4 referring to other experimental result, and initial axial force N was made to be N=6.86 kN referring to the dead load. The friction was assumed by the Coulomb friction characteristics.

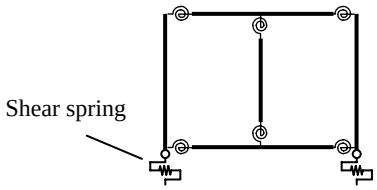

Figure 11 The modeling of the slip property in the column base
(X13 plane of structure)

In the case of inputting BCJ-L2 wave (300gal) into the Model B (waist tie beam type) for the short edge direction, time history response of the story deformation angle at plane of structure X1 and X13 are shown in Figures 12 and Figures 13. In these figures, the black line shows analysis value, and the gray line shows experimental value.

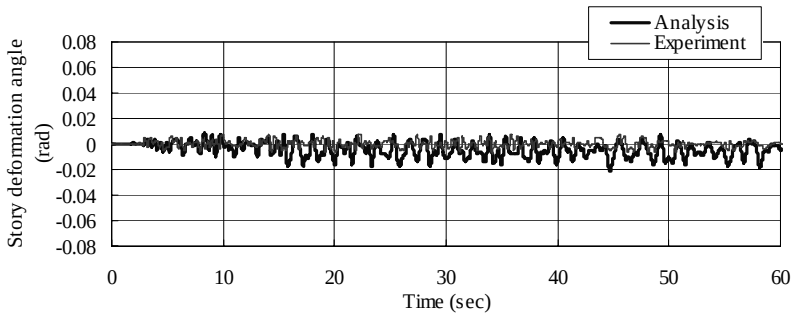

Figure 12 Time history response of the story deformation angle at plane of structure X1,
Model B (waist tie beam type), (BCJ-L2, 300gal)

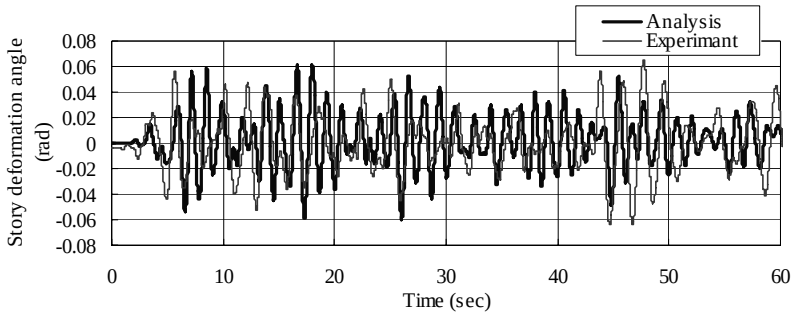

Figure 13 Time history response of the story deformation angle at plane of structure X13, Model B (waist tie beam type), (BCJ-L2, 300gal)

Time history response of the slip movement for the short edge direction at the X1Y5 column base is shown in Figures 14. In this figure, the black line shows analysis value, and the gray line shows experimental value. The behavior of slip movement on the present analysis is different from the experimental measurement as shown in this figure. It is considered that the effect of the slip phenomenon with the rocking vibration can not be represented by present formulation based on shear spring element for mud wall.

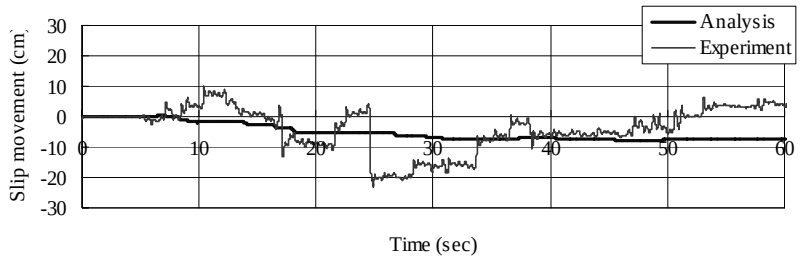

Figure 14 Time history response of the slip movement of X1Y5 column base for short edge direction, Model B(waist tie beam type), (BCJ-L2, 300gal)

5. CONCLUSIONS

In this paper, we presented earthquake response analysis of traditional wooden building for full-scale vibration test applying three dimensional frame analysis models with semi-rigid connections, and investigated the response characteristics of the present analysis models. As the result, it was confirmed that the effectiveness of modeling for the sill beam model wooden building by the rotation spring element at the element ends and shear spring element for mud wall. However, for waist beam model wooden building, the behavior of slip movement on the present analysis is different from the experimental measurement. Therefore, it is not sufficient to simulate the waist tie beam model wooden buildings by present method. Hereafter, it is necessary to propose the modeling which can appropriately consider the effect of the rocking in addition to the shear.

REFERENCES

Suzuki, Y., Gotou, M., Saito, Y., Kamada, T., Shimizu, H., and Nakamura, I., (2007). Vibration tests of traditional wooden buildings by E-Defense shaking table Part 1 Objectives and outline of vibration tests. *Summaries of Technical Papers of Annual Meeting Architectural Institute of Japan* **C-2**, 515-516. (in Japanese)

Faris G.A., Al-Bermani, and Kitipornchai, S., (1992). Elastoplastic Nonlinear Analysis of Flexibly Jointed Space Frames, *Journal of Structural Engineering*, **vol. 118, No. 1**, pp. 108-127.

Li, G., and Shen, Z., (1995). A Unified Matrix Approach for Nonlinear Analysis of Steel Frames Subjected to Wind or Earthquakes , *Computers & Structures*, **vol. 54 , No. 2** ,315-325.

Suarez, L. E., Singh, M. P., and Matheu, E. E., (1996). Seismic Response of Structural Frameworks with Flexible Connections , *Computers & Structures*, **vol. 58 , No.1** ,27-41.

Davison, J. B., Kirby, P. A., and Nethercot, D. A., (1987). Rotational Stiffness Characteristics of Steel Beam-to-Column Connections, *J. Construct. Steel Research*, **vol. 8**, 17-54.

Fujitani, Y., Fujii, D., and Matsumoto, S., (1997). Elasto-plastic Earthquake Response Analysis of Framed Structure with Semi-rigid Connections, *International Scientific Conference, Challenges to Civil and Mechanical Engineering in 2000 and beyond, Technical University of Wroclaw Institute of Building Engineering, Poland*, **Vol.2**, 405-414.

Shojo, N., Fujitani, Y., Matsumoto, S., Ohno, Y., and Ohash, Y., (2005). Study on dynamic characteristics of timber frame structure by microtremor measurements, *Archives of Civil and Mechanical Engineering*, Vol.V, No.3, 59-67.

Matsumoto, S., and Fujitani, Y., (2007). Study on analytical method for wooden structures with sheathed shear walls, *International Conference on Computational Methods, International Conference Center Hiroshima, Japan*, **CD-ROM**, 36.